Original Research

The chaperone system in glioblastoma multiforme and derived cell lines: diagnostic and mechanistic implications

Giusi Alberti[1,‡], Claudia Campanella[1,‡], Letizia Paladino[1,2], Rossana Porcasi[3],
Celeste Caruso Bavisotto[1], Alessandro Pitruzzella[1,4], Francesca Graziano[5],
Ada Maria Florena[3], Antonina Argo[6], Everly Conway de Macario[7], Alberto JL Macario[2,7],
Francesco Cappello[1,2], Fabio Bucchieri[1,8], Rosario Barone[1,§], Francesca Rappa[1,*,§]

[1]Department of Biomedicine, Neurosciences and Advanced Diagnostics (BiND), University of Palermo, 90127 Palermo, Italy
[2]Euro-Mediterranean Institutes of Science and Technology (IEMEST), 90139 Palermo, Italy
[3]Department of Sciences for the Promotion of Health and Mother and Child Care, Anatomic Pathology, University of Palermo, 90127 Palermo, Italy
[4]Consortium of Caltanissetta, 93100 Caltanissetta, Italy
[5]Department of Neurosurgery, Highly Specialized Hospital and of National Importance "Garibaldi", 95122 Catania, Italy
[6]Department of Health Promotion, Mother and Child Care, Section of Legal Medicine, University of Palermo, 90127 Palermo, Italy
[7]Department of Microbiology and Immunology, School of Medicine, University of Maryland at Baltimore-Institute of Marine and Environmental Technology (IMET), Baltimore, MD 21202, USA
[8]Institute for Biomedical Research and Innovation (IRIB), National Research Council of Italy (CNR), 90100 Palermo, Italy
*Correspondence: francesca.rappa@unipa.it (Francesca Rappa)
‡These authors share the first authorship.
§These authors share the last authorship.
Academic Editor: Graham Pawelec
Submitted: 28 December 2021   Revised: 24 January 2022   Accepted: 25 January 2022   Published: 15 March 2022

Abstract

Background: Glioblastoma multiforme (GBM) is the most common and malignant primary brain tumor in adults. Novel treatments are needed to counteract the molecular mechanisms of GBM growth and drug resistance. The chaperone system (CS) members are typically cytoprotective but some, termed Hsp, can become pathogenic and participate in carcinogenesis, along with the vascular endothelial growth factor (VEGF), and we investigated them in GBM biopsies and derived cell lines. The objectives were to identify diagnostic-prognostic biomarkers and gather information for developing chaperonotherapy. **Methods**: Cell lines from GBMs were established, characterized (morphology, growth characteristics, and specific markers), and stored. Chaperones and angiogenic factors [Hsp10, Hsp27, Hsp60, Hsp70, Hsp90, FLT-1 (VEGFR-1), FLK1 (KDR, VEGFR-2), and FLT-4 (VEGFR-3)] were observed in cells by immunofluorescence while the chaperones were measured in tumor tissue by immunohistochemistry. **Results**: Four cell lines were derived from four different GBMs; the cells were spindle shaped or polygonal and grew at high rates as adherent monolayers or clusters without evidence of contact inhibition. The astrocyte-specific glial fibrillary acidic protein (GFAP); and the neuronal NSE, malignancy VIM, and proliferation PCNA, markers were determined. The cells expressed GFAP but no NSE, indicating that they were primary glioblastoma cell lines, with high levels of Hsp10, Hsp27, Hsp60, Hsp90, and Flk1; and low levels of Hsp70, Flt1, and Flt4. **Conclusions**: Four cell lines were established derived from four out of ten GBM tumors studied. The cell lines showed intense positivity for chaperones studied and factors connected to malignancy and the tumors showed increased levels of chaperones, making them potential diagnostic-prognostic biomarkers and targets for anti-cancer compounds.

Keywords: glioblastoma multiforme (GBM); chaperone system (CS); heat shock protein (Hsp); vascular endothelial growth factor (VEGF); GMB cell lines

1. Introduction

Glioblastoma multiforme (GBM) develops from astrocytes and is the most aggressive primary cancer in human brain. GBM rarely metastasizes, it induces death through invasion of normal brain tissue and by resisting therapies. The 2016 World Health Organization (WHO) Classification of CNS Tumors combines histological and molecular parameters to define various types of gliomas [1]. Diffuse glioblastomas are separated into two groups, with and without mutation of the isocitrate dehydrogenase

(IDH) gene, namely, WHO grade IV with and without IDH mutation [2]. These two groups of gliomas have different histopathological features, modes of progression, and prognoses [3]. IDH mutation frequently occurs in secondary glioblastomas, which grow slowly and have a favorable prognosis. The wild-type IDH occurs in older patients in the absence of any lower-grade precursor and have a worse prognosis [4]. Prognosis and clinical progression also differ significantly within the groups, indicating that there are other factors still to be identified that distinguish tumor sub-

groups. In addition, the location and size of glial tumors determine the clinical presentation, requiring personalized monitoring and treatment strategies.

The distinctive feature of GMB is the recurrence and short survival time after aggressive therapies. This is due to the "angiogenic switch", consisting of the formation of a dense network of vessels tortuous and hyperpermeable, with production of pro-angiogenic factors, resulting in the uncontrolled proliferation, infiltration, and progression of the tumor. Angiogenesis is driven by mechanisms that lead to activation of the vascular endothelial growth factor (VEGF), one of the most important regulators of tumor growth [5]. The critical role of VEGF in angiogenesis makes it an appealing target for therapeutics. Preclinical data and early clinical trials with agents targeting VEGF prolonged patient survival; however, acquired anti-medication resistance and incomplete VEGF blockade made clear that other more efficacious therapies for GBM would have to be developed [6,7].

New avenues for research and for developing novel tools for prognostication and treatment of GBM have been opened by progression in the knowledge of the chaperone system (CS) and its functions as a physiological entity in health and disease, including tumors. The CS of an organism, e.g., a human, is composed of molecular chaperones, chaperone co-factors, co-chaperones, and chaperone receptors and interactors [8]. Molecular chaperones, the chief members of the CS, are proteins classified according to molecular weight into groups, encompassing the following ranges (in kDa): $\leq$34; 35–54; 55–64; 65–80; 81–99; 100–199; and $\geq$200; within these groups are families of phylogenetically related molecules termed heat shock protein (Hsp), such as the Small Hsp (those with the alpha-crystallin motif), Hsp40/DnaJ, Hsp70/DnaK, and Hsp90 families; and others, e.g., the CCT (Chaperoning-containing TCP1) family [8]. The canonical role of the CS is maintenance of protein homeostasis, but it also has non-canonical functions pertaining to immunity, inflammation, and cancer [9–14]. In mitochondria, Hsp10 works with Hsp60 in forming a protein-folding machine, which is essential for cell life and survival. In some types of cancer, cells overexpress Hsp10, which accumulates in the cytoplasm, probably involved in neoplastic transformation [15,16]. Hsp27 is another chaperone that is increased in various types of cancer [17–19]. In glioma cell lines, Hsp27 is involved in a malignant phenotype, including proliferation, migration, and invasion [20]. Hsp60 is overexpressed in high-grade gliomas, and interacts with Hsp90 and co-factors, modulating tumor growth by preventing apoptosis *in vivo* [21]. Upregulation of members of the Hsp70 family has been observed in many tumors and a positive correlation with the WHO tumor grade has been reported for glioma [22]. Hsp70 is involved in the cancer-cell response to hypoxia, as its chaperoning activity is required for the folding, stabilization, and nuclear translocation of HIF (hypoxia-inducible factor) [23]. Cancer cells use the Hsp90 chaperone machinery to protect mutated and overexpressed oncoproteins, e.g., HIF and VEGF, from misfolding and degradation favoring cancer-cell survival [24]. GBM contains hypoxia niches that provide an environment favorable to the maintenance of stemness of the Glioblastoma Stem-like Cell (GSC) and, Hsp90 has been identified in the cells of this tumoral region co-localizing with stem-cell markers and HIF. Hsp90 is also considered a key protein for GBM cell migration and invasiveness, as well as modulation of survival and apoptosis [25].

The data briefly discussed above and many others in the literature support the notion that the CS system is involved in carcinogenesis, both against and for cancer development. Although the CS system components, particularly the molecular chaperones, are typically cytoprotective, if abnormal they can cause diseases, the chaperonopathies [26]. Therefore, it is pertinent to ask about the role of chaperones in GBM as possible biomarkers useful for differential diagnosis, prognostication, and patient follow up. Furthermore, it is highly likely that by revealing the quantitative and distribution patterns of chaperones in GBM in relation to clinical manifestations, response to treatment, and other pathological parameters, will provide clues for developing efficacious treatments targeting the chaperones, namely chaperonotherapy [27,28]. Consequently, we have been studying the CS in various cancers and, in the research reported here, we conducted an immunohistochemical evaluation in GBM tissue samples of the chaperones Hsp10, Hsp27, Hsp60, Hsp70, and Hsp90. In parallel, we also studied other molecules pertinent to GBM biology, such as Flt1 (VEGFR-1), Flk1 (KDR, VEGFR-2), and Flt4 (VEGFR-3) in primary glioblastoma cell lines derived from patient biopsies. The immediate objective of this project is to reveal features useful for tumor identification and differential diagnosis, while the long-term goal is to accumulate information that could serve as a platform for the development of therapeutic means targeting the pathogenic chaperones.

2. Materials and methods

2.1 Patients and tissue samples

The patients enrolled in this study underwent surgery for supratentorial, hemispheric GBM at the Neurosurgery Department, Policlinico P. Giaccone, University of Palermo. In all cases, total tumor removal was done-namely, a resection of the entire contrast-enhancing lesion confirmed by MRI. All patients gave their written informed consent to study participation. This study was approved by the Ethics Committee of University Hospital AUOP Paolo Giaccone of Palermo (number 11/2018) in accordance with current legislation and the ethical standards laid down in the 1964 Declaration of Helsinki and its later amendments. The samples were collected between 2019 and 2021; tumor diagnosis was performed according to the fourth edition of the WHO classification of tumors of the central nervous

Table 1. Diagnostic analysis of enrolled patients for IDH1, Ki67, and synaptophysin.

Patients	Sex	Anatomical site	IDH1[1]	Ki67 percentage	Synaptophysin
1	M	Left frontal lobe	–	67.17	
2	F	Left parieto-occipital region	+	67.25	
3	F	Right frontal lobe	NOS	67.25	
4	F	Right frontal lobe	NOS	67.40	
5	M	Right frontal lobe insular region	+/–	67.10	
6	F	Left frontal lobe	–	67.40	Negative
7	M	Left frontal lobe	–	67.40	
8	M	Left frontal lobe	–	60.40	
9	F	Right temporal lobe	+	60.20	
10	M	Right temporal lobe	+	67.20	

[1] Abbreviations and symbols: IDH1, isocitrate dehydrogenase (NADP(+)) 1; Ki67, antigen identified by monoclonal antibody Ki-67, currently named MKI67; M, male; F, female; –, negative; +, positive; NOS, Not Otherwise Specified.

system. In our study, 10 patients with glioblastoma were enrolled at the Policlinico P. Giaccone and tissue biopsy samples were obtained from nine of them. Cell lines were established from 4 of the 9 samples. The mean age of the patients was 57.75 years (ranging from 53 to 64) and their clinical characteristics such as anatomical site, isocitrate dehydrogenase (NADP(+)) 1 IDH1 wild type (WT) or mutant, Ki67, and synaptophysin are summarized in Table 1. IDH mutations, Ki67, p53 and synaptophysin were determined in all glioblastoma cases from the Institute of Pathological Anatomy. In addition, 10 non-pathological samples of cortex from age-matched subjects, were used for comparative analysis, obtained from U.O.S. Forensic Medicine, Policlinico P. Giaccone.

2.2 Immunohistochemistry

Immunohistochemical staining was performed using formalin-fixed paraffin-embedded blocks. Briefly, 4-μm-thick tissue sections, obtained by microtome cutting, were deparaffinized in xylene and hydrated by immersing in a series of graded ethanol. Antigen retrieval was performed placing the sections in epitope retrieval solution (0.01 M citrate buffer, pH 6.0) for 8 min and immersed for 8 min in acetone at –20 °C to prevent the detachment of the sections from the slide. After washing the sections with PBS (phosphate buffered saline, pH 7.4) for 5 min at 22 °C, the immunohistochemical reaction was performed by the streptavidin–biotin complex method using a Histostain®-Plus Third Gen IHC Detection Kit (Life Technologies, Frederik, MD, USA; Cat. No. 85–9073). The sections were treated for 5 min with Peroxidase Quenching Solution (reagent A of Histostain®-Plus 3rd Gen IHC Detection Kit, Invitrogen) to inhibit endogenous peroxidase activity. Endogenous peroxidase was inhibited by immersing the sections in 0.3% hydrogen peroxide for 10 min. Sections were then incubated with the primary antibody reported in Table 2. The immunohistochemistry procedure

was performed as described previously [29]. Appropriate negative controls were run concurrently for each reaction. Nuclear counterstaining was performed using hematoxylin (Hematoxylin aqueous formula, nREF 05-06012/LN. Cat. No. S2020, Bio-Optica, Milano, Italy). Finally, the sections were observed with an optical microscope (Microscope Axioscope 5/7 KMAT, Carl Zeiss, Oberkochen, Germany) connected to a digital camera (Microscopy Camera Axiocam 208 color, Carl Zeiss, Oberkochen, Germany). All observations were performed by two independent observers (F.C. and F.R.). The percentage of positive cells was calculated in a high-power field (HPF) (magnification 400×) and repeated for 10 HPFs. The arithmetic mean ± standard deviation of counts was used for statistical analysis.

2.3 Establishment of cell lines

Tumor tissue was collected during resection and transferred cooled to the laboratory. Under sterile conditions, it was rinsed in PBS and, subsequently, obvious vessels, coagulated blood, and necrotic tissue were removed. Each tumor specimen was dissociated into small pieces, using scalpels, and dissociated further enzymatically by incubation with Collagenase Type II (250 U/mL, Sigma Aldrich, St. Louis, MO, USA), 0.25% of trypsin (Thermo Fisher, Waltham, MA, USA) in PBS at 37 °C for 18 h under shaking. At the end the incubation period, trypsin activation was stopped by adding medium containing 10% fetal bovine serum (FBS, Thermo Fisher Scientific). Centrifugation at 300× g for 5 min at 4 °C was performed to recover the cells from the enzyme solution and resuspended in Dulbecco's Modified Eagle's Medium (DMEM 1X, Thermo Fisher Scientific), supplemented with 10% FBS, and then the cells were filtered with a 70 μm cell strainer. The cells were washed by centrifugation and seeded in cell culture flasks with a medium composed of DMEM, 10% FBS, 100 U/mL penicillin (Thermo Fisher Scientific), and 0.1 mg/mL strep-

Table 2. Primary antibodies used for immunohistochemistry and immunofluorescence.

Method	Antigen	Antibody	Clone	Supplier	Dilution
IHC/IF[1]	Hsp10	Mouse monoclonal	clone D-8	Santa Cruz Biotechnology, Dallas, TX, USA	IHC: 1:100 IF: 1:50
IHC/IF	Hsp27	Goat polyclonal	clone F- 4	Santa Cruz Biotechnology	IHC: 1:200 IF: 1:50
IHC/IF	Hsp60	Rabbit polyclonal	H-300	Santa Cruz Biotechnology	IHC: 1:300 IF: 1:50
IHC/IF	Hsp70	Mouse monoclonal	5A5	Abacam, Cambridge, UK	IHC: 1:100 IF: 1:50
IHC/IF	Hsp90	Mouse monoclonal	ab13492	Abcam	IHC: 1:200 IF: 1:50
IF	GFAP	Mouse monoclonal	2E1	Santa Cruz Biotechnology	1:50
IF	NSE	Mouse monoclonal	MRQ-55	Ventana Medical System, Tucson, Arizona, USA	1:50
IF	VIM	Mouse monoclonal	V9	Biocare, Dallas, USA	1:50
IF	β-tubulin	Mouse monoclonal	TUB 2.1	Sigma-Aldrich, St Louis, MO, USA	1:50
IF	ALDH1	Mouse monolconal	H-8	Santa Cruz Biotechnology	1:50
IF	PCNA	Mouse monoclonal	F-2	Santa Cruz Biotechnology	1:50
IF	FLT-1	Rabbit polyclonal	C-17	Santa Cruz Biotechnology	1:50
IF	FLK-1	Mous emonoclonal	A-3	Santa Cruz Biotechnology	1:50
IF	FLT-4	Rabbit polyclonal	C-20	Santa Cruz Biotechnology	1:50

[1] Abbreviations: IHC, immunohistochemisry; IF, immunofluorescence.

tomycin (Thermo Fisher Scientific) at 5% CO_2 atmosphere at 37 °C. For suspension cultures and adherent cultures, T25 cell culture flasks were used. After a 1-day resting phase, the culture supernatant was removed, the cells were washed with PBS 1X (if there was cellular debris in the culture), and new culture medium was added. Change of culture medium and microscopic monitoring (phase contrast) were performed every 2 days. Aliquots of the cell lines have been stored frozen for future studies.

2.4 Tumor cell culture

We used the cell line G166, isolated from malignant glioma (ISENET Biobanking Cell Lines) that show stem cell properties and with the capability of initiating high grade gliomas after xenograft. Cells were grown in serum-free complete medium (Euromed-N, EuroClone; code ECM0883LD), with supplements: 2% B27 (GIBCO; code 17504-044), 1% N2 (GIBCO; code 17502-048), 20 ng/mL epidermal growth factor (EGF, Peprotech; code 100-15) added fresh; 20 ng/mL basic fibroblast growth factor (FGF2, Peprotech; code 100-18B) fresh added; on the laminin coating at 1 μg/mL (Invitrogen; code 23017-015). The cells were split once per week after dissociation with Accutase solution (Sigma Aldrich) and centrifugation at $1000\times$ g for 3 min, and seeded in laminin-coated flasks with gentle shaking 2 h at 22 °C. The cells were incubated at 37 °C in a humidified atmosphere with 5% CO_2 until confluence in monolayer.

2.5 Hematoxylin-Eosin staining

Five thousand cells per well were plated in chamber slides and allowed to attach and proliferate for 24 or 48 h. After fixation (ice-cold methanol for 30 min, Carl Roth, Karlsruhe, Germany) the cells were stained with Hematoxylin-Eosin (H&E), using stain in hematoxylin solution (Papanicolaou Harris Hematoxylin, Bio-Optica:

code: 05-12011) for 1 h at 22 °C; followed by counterstain with Eosin Y (Eosin Y aqueous solution 1%, BioOptica; code: 05-M10002) for 1.5 min. The slides were then mounted with histologic mounting medium and a cover glass, and finally observed with an optical microscope (Microscope Axioscope 5/7 KMAT, Carl Zeiss, Oberkochen, Germany) connected to a digital camera (Microscopy Camera Axiocam 208 color, Carl Zeiss).

2.6 Immunofluorescence and confocal microscopy

For immunofluorescence, the cells were placed in eight-well chamber slides, cultured for 24 h and fixed with ice cold methanol for 30 min. The fixed cells were washed with PBS pH 7.4 and then incubated with unmasking solution (trisodium citrate 10 mM, 0.05% Tween 20, pH 6) for 10 min at 22 °C. After rinsing twice with PBS, the cells were blocked with 3% (w/v) bovine serum albumin (BSA, Sigma Aldrich) in PBS for 30 min at 22 °C and incubated in a humidified chamber overnight at 4 °C with primary antibodies (Table 2). The day after, the cells were washed twice in PBS and were incubated with a fluorescent secondary antibody (anti-rabbit IgG-FITC antibody produced in goat, F0382, Sigma-Aldrich, 1:100 dilution; anti-mouse IgG-TRITC antibody produced in goat, T5393, Sigma-Aldrich, 1:100 dilution; anti-rabbit IgG-Atto 647 antibody produced in goat, 40839, Sigma-Aldrich, 1:150 dilution; anti-mouse IgG-Atto 488 antibody produced in goat, 62197, Sigma-Aldrich, 1:150 dilution). The nuclei were counterstained with DAPI 33342 (1:1000, Sigma-Aldrich) for 15 min at 22 °C. Finally, the slides were covered with drops of PBS and mounted with coverslips. The images were captured using a Leica Confocal Microscope TCS SP8 (Leica Microsystems). Cell lines with cells immunopositive for GFAP and negative for NSE were defined as "primary glioblastoma cell lines".

2.7 Data analysis

Statistical analyses were carried out using the Graph-Pad Prism 4.0 package (GraphPad Inc., San Diego, CA, USA). Comparisons of immunohistochemical evaluations were made by using Student's t-test. All data are presented as the mean $\pm$ SD, and the level of statistical significance was set at $p \leq 0.05$.

3. Results

3.1 Immunohistochemistry: quantity and distribution of molecular chaperones in GBM tissue

Hsp10 immunopositivity was cytoplasmic in glioblastoma cells with an average percentage of positive cells of 61.6 ± 1.8, while in the control tissue the Hsp10 positivity was $5.5 \pm 0.6\%$ ($p < 0.001$) (Figs. 1,2). The average percentage of Hsp27 positive cells in GBM was $86.5 \pm 2.1\%$ while in control samples was $5.7 \pm 0.7\%$ ($p < 0.001$) (Figs. 1,2). The immunolocalization of Hsp27 was cytoplasmic. The cells positive for Hsp60 were $66.5 \pm 2.1\%$ in GBM and 5.3 ± 0.3 in control group, with a cytoplasmic positivity ($p < 0.001$) (Figs. 1,2). The Hsp70 positive cells in GBM and CTR were present but at low levels, with an average percentage of 4.2 ± 0.57 in the GBM and 4 ± 0.7 in the CTR group, with no significant difference between these two groups (Figs. 1,2). Hsp90 positive cells were $72 \pm 2.9\%$ in GBM and 4 ± 0.55 in CTR samples ($p < 0.001$) (Figs. 1,2).

3.2 Culture efficiency

The tumor-tissue sample from one of the 10 patients did not pass the short-term primary stage of culture. Of the other nine glioblastoma-tissue samples, five did not attach after disaggregation and did not grow. The other four samples, however, did grow from the start and yielded self-replicating passageable cell lines. This diversity of reaction to explantation probably reflects the area of the tumor from which the sample originates. If the sample is taken from a necrotic area, there are no cells, or extremely few that can grow in the cultures. If the tumor sample originates in a transitional area between necrosis and proliferation, cultivation is possible, but often large amounts of cell debris are present in the culture causing reducing cell viability still more. The presence of erythrocytes in the culture of samples with a high blood supply also leads to cell death. The four cell lines described here were designated GBM1, GBM2, GBM3, and GBM4. The time from explantation (p0) of the tumor samples to the first sub-cultivation step (p1) differed between the primary cell lines: one week for GBM2 and GBM3, and two and three weeks for GBM1 and GBM, respectively.

3.3 Morphological and growth characteristics of the four new cell lines

The new cell lines showed two types of growth: (a) monolayer with the cells growing side by side; and (b) fo-cal with the cells growing in clusters or islands connected by cell protrusions. The commercial cell line G166 grew as a monolayer. In slides stained with Hematoxylin-Eosin, the primary cell lines showed three different cellular shapes: polygonal (Fig. 3A,B), spindle or glia-like (Fig. 3C–F), and amorphous with cellular protrusions (Fig. 3G,H). Multinucleated giant cells were also present at low frequency. The G166 cell line showed a glia-like morphology (Fig. 3I,L). Aliquots of the cell lines have been stored frozen and they recovered and grew well after thawing.

3.4 Immunofluorescence: demonstration of GBM markers and mapping of chaperones in the new cell lines

To establish criteria for the definition of primary glioblastoma cell lines and to ascertain whether the glioblastoma-derived primary cell lines have similarities to glioblastoma tissue, we resorted to immunofluorescence staining for markers used in glioma diagnosis with confocal microscopy, comparing our cell lines with the G166 line. The primary cell lines were tested to determine the presence of GFAP, which is characteristic of astrocytes or glial cells [30]; Vimentin, a neuroepithelial precursor marker [31]; β-tubulin, a marker associated with tumor resistance to microtubule-targeting agents (MTAs) [32]; neuron-specific enolase (NSE), a neuronal marker [33]; and ALDH1, a stem-cell marker [34]. Positive immunoreactivities for GFAP, Vimentin, and β-tubulin, and negative immunoreactivity for NSE were detected in our four cell lines, as expected from GBM-derived cell lines (Fig. 4). The levels of GFAP varied being higher in GBM2, GBM3 and GBM4 compared to GBM1. The cell lines did not show staining for NSE except for GBM4, which showed a weak positive reaction. ALDH1 immunoreactivity was found in GBM1 (very weak), GBM2, and G166 cell lines, but the other cell lines were negative (Fig. 4). PCNA was present in all lines (Fig. 4). PCNA immunoreactivity was mostly confined to nuclei (diffuse or granular stained nuclei) in GBM1, GBM2 and GBM4 primary cell lines, whereas cytoplasmic staining was seen in GBM2, GBM3, GBM4, and G166 cell lines.

The immunopositivity for the molecular chaperone Hsp10 was observed in the cytoplasm of the primary cell lines (Fig. 5) and the cell line that showed the most intense reaction was GBM3, which derived from the youngest patient in the group studied. Hsp27 immunopositivity was intense in GBM2 (this line derived from the GBM patient with the shortest survival after surgery) and occurred also in GBM1, GBM3, GBM4 (derived from GBM patients with longer survival period after surgery) (Fig. 5). Hsp27 staining in the tumor tissue was not significantly different among the GBM patients. The Hsp60 reaction showed a granular and diffuse cytoplasmic positivity in our four GBM cell lines and in the G116 line (Fig. 5). The immunopositivity of Hsp70 was very low or absent in our four cell lines but it was present at very low levels in the G166 cell line (Fig. 5). These results obtained with immunofluorescence are in line
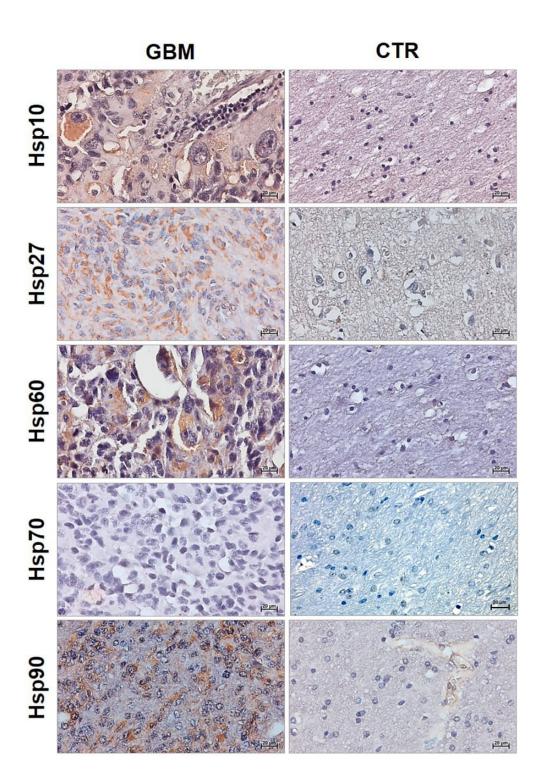
Fig. 1. Immunohistochemical demonstration of molecular chaperones in GBM tissue. Representative images for Hsp10, Hsp27, Hsp60, Hsp70 and Hsp90 in glioblastoma multiforme (GBM) and control (CTR) tissues. The staining pattern for the Hsp10, Hsp27, Hsp60, and Hsp90 proteins was cytoplasmic, with strong intensity in GBM tissue. Low immunopositivity of Hsp70 in the cytoplasm in GBM tissue like that of CTR. Magnification $400\times$, scale bar 20 μm.

with the immunohistochemical data (Figs. 1,2). Our four cell lines and G166 were positive for Hsp90 (Fig. 5). G166 cell line showed cytoplasmic positivity for all Hsps, including Hsp70 (Fig. 5).

Illustrative images of the immunofluorescence mapping of the VEGFR1 (Flt1), VEGR2 (Flk1), and VEGFR3 (Flt4) are shown in Fig. 6. The four GBM lines and the G166 cell line were positive for VEGFR-1 (Flt1) and for

Fig. 2. The chaperones tested except for Hsp70 were augmented in GBM by comparison with the control tissue. The histograms show the percentage of immunopositivity for Hsp10, Hsp27, Hsp60, Hsp70, and Hsp90 in GBM and CTR tissues. Data are presented as the mean $\pm$ SD. * $p < 0.0001$.

VEGFR-2 (Flk1) in the cytoplasm. VEGFR-3 (Flt4) occurred in the G166 cell line and in our cell lines GBM2, 3, and 4 but was undetectable in GBM1.

4. Discussion

GBMs show a remarkable molecular heterogeneity that defeats the effectiveness of therapeutic approaches that are not patient specific. Understanding the cellular and molecular mechanisms of malignant growth in GBM will be instrumental for identifying new targets for treatment that could guide the development of personalized therapies. In this study, we focused on molecular chaperones. These are the chief members of the CS and are known to play key roles in carcinogenesis, both anti- and pro-tumoral roles

[11,14,29,35–39]. They are also promising candidates as biomarkers for differential diagnosis, prognostication, and patient follow up. We evaluated by immunohistochemistry and immunofluorescence the presence and subcellular localization of the chaperones Hsp10, Hsp27, Hsp60, Hsp70, and Hsp90 in biopsies of ten GBMs. Our experiments showed a high Hsp27 immunopositivity in the cytosol of all GBMs, by comparison with normal tissue. Hsp27 protein levels were higher in biopsies from GBM cases with short survival, a trend found also in other tumors, suggesting that elevated levels of Hsp27 may predict poor prognosis [40]. The immunopositivity for Hsp10 and Hsp60 was also elevated in the GBM tissue in contrast with the normal controls, with Hsp60 present in the cytoplasm, as shown
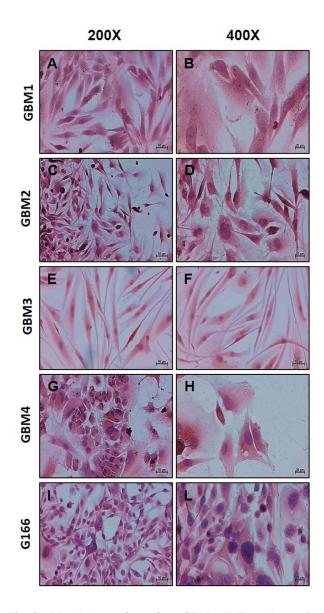
Fig. 3. Morphology of our four GBM cell lines along with that of the commercially available G166 line revealed by Haematoxylin-Eosin staining. Cell lines images: GBM1 (A: GBM1 magnification 200×; B: GBM1 magnification 400×), GBM2 (C: GBM2 magnification 200×; D: GBM2 magnification 400×), GBM3 (E: GBM3 magnification 200×; F: GBM3 magnification 400×), GBM4 (G: GBM4 magnification 200×; H: GBM4 magnification 400×), G166 (I: G166 magnification 200×; L: G166 magnification 400×). Morphological heterogeneity within each line is evident, with some predominance of spindle cells in GBM1, 2, and 3; and with star-shaped and irregularly shaped cells in the GBM4 line.

for other types of solid tumors, in which the levels of this chaperonin correlated with tumor progression [15,41,42]. Hsp60 and Hsp10 are typically mitochondrial molecules, therefore, our finding them in the cytoplasm of GBM cells supports the notion that the chaperonins augment in the cy-

tosol of tumor cells and are markers of malignancy. The chaperone Hsp70 have been found increased or decreased in human cancers by comparison with healthy control tissues [43–45]. An inverse correlation between Hsp70 levels and prognosis has been observed in some cancers [35,46]. In contrast to these findings, we did not detect a clear positivity reaction for Hsp70 in the GBM tissues we describe here, although we found low but still detectable levels of this chaperone in the commercially available stem line G166. This probably indicates that in this stem-cell line, Hsp70 is in the stem-cell nuclei, but it is absent in the other cell lines, in which stem cells have not been demonstrated. Hsp90 was detected many years ago in GBM [47,48]. In our study, we observed a higher Hsp90 immunopositivity in tumor tissue compared to normal brain tissue. All the observations on the chaperones in the tumor and derived cell lines by immunohistochemistry were confirmed by immunofluorescence.

The four cell lines reported here show some morphological heterogeneity, but most cells have a spindle- or glia-like shape and there are also few multinucleated giant cells. The proportion of these cell types remained unchanged during cultivation and successive passages. The morphological heterogeneity of our cell lines reflects that of the original GBM tumors, which is characteristic of them. The cell lines displayed the markers of neuroglia, for instance GFAP and VIM, indicating that the cells derive from transformed glial cells. Available information suggests that the expression of GFAP and VIM is mostly confined to glial-derived tumors, and that VIM can potentially be a useful marker for distinguishing undifferentiated GFAP-negative glial tumors. Other markers we measured in the cell lines are NSE, ALDH1, and PCNA. We observed no reaction for NSE, a low positivity for ALDH1, and positivity for PCNA. The absence of NSE, a neuronal marker, confirms the non-neuronal origin of the cell lines. ALDH1 has been suggested as a novel stem-cell marker in a small series of human glioblastomas [34], but the expression and functions of ALDH1 in the central nervous system (CNS) and its tumors are largely unknown. Our experiments showed that the primary cell lines do not have stem cell characteristics in contrast with G166, which showed immunopositivity for ALDHI. The immunofluorescence results with anti-PCNA antibodies indicate that the cell lines do show the parameters of malignancy that PCNA represent.

We observed positivity for Hsp27 in the cytosol of the cells and a diffuse positivity for Hsp60 and Hsp10 in the cytoplasm of all cell lines. The positive immunofluorescence reaction of Hsp10 and Hsp60 in the cytosol of the cells matched results obtained by immunohistochemistry in the tumor tissues. The fact that these chaperones were elevated from the first passages of cell growth, and remained elevated during cultivation, suggests that they are implicated in the onset and progression of carcinogenic mechanisms. It is possible that the increase in the amounts of Hsp27, Hsp10,
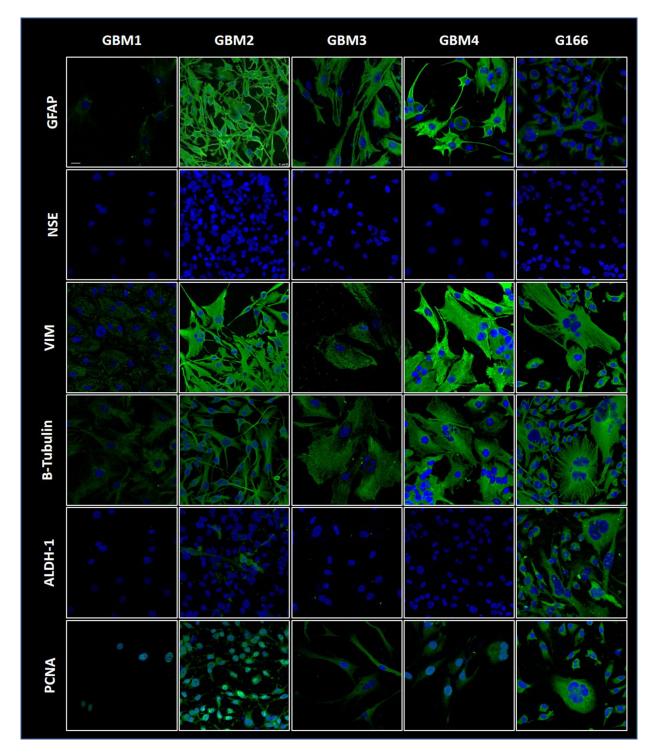
Fig. 4. GBM markers detected by immunofluorescence in the four cell lines along with the G166 line. GFAP, VIM, β-tubulin, ALDH1, and PCNA are present in our four lines at diverse levels, a diversity made apparent by comparing our cells lines with one another and with the commercially available G166 line. NSE was absent in the four cell lines and in G166. Specific primary antibodies for each marker and secondary antibody labelled with FITC (green fluorescence in the figure) were used and the cell nuclei (blue) were stained with DAPI. Magnification 400×, scale bar 20 μm.

and Hsp60 reflects the exaggerated requirements of tumor cells for new proteins correctly folded caused by their accelerated metabolism and growth and replication rates. The prognostic value of Hsp90 levels depends on the tumor type [48]. Hsp90 is often increased and associated with poor prognosis in various tumors, including GBM [49–54]. We found high levels of Hsp90 in the GBM2 and GMB4 cell lines with a cytoplasmic localization, in all passages. High
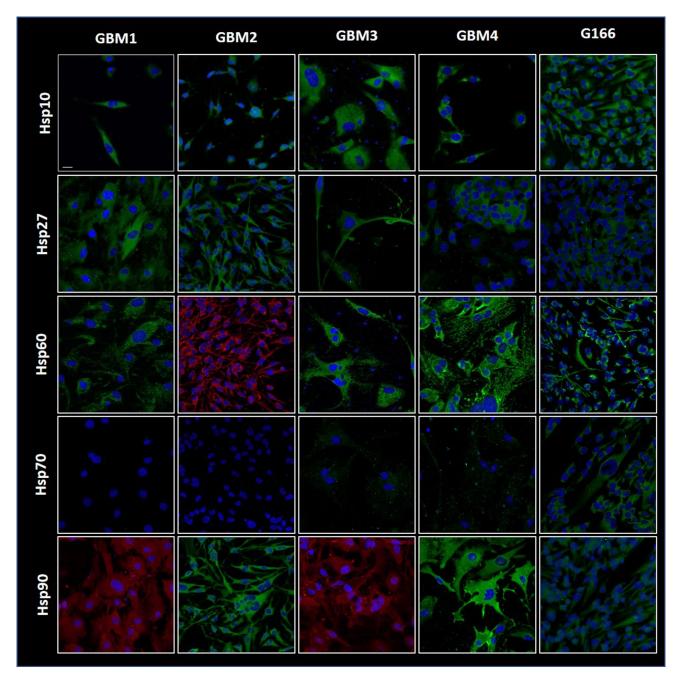
Fig. 5. Demonstration by immunofluorescence of CS components in the GBM cell lines. The chaperones Hsp10, Hsp27, Hsp60, and Hsp90 were present at diverse levels in our four cell lines, and in the G166 line. Hsp70 was at very low levels in the four cell lines, comparable to that in C166 or lower. All the chaperones were present in G166. Specific primary antibodies for the chaperones and secondary antibody conjugated with FITC (green fluorescence in the figure) or with TRITC (red fluorescence in the figure) were used, and the cell nuclei (blue) were stained with DAPI. Magnification 400×, scale bar 20 μm.

levels of Hsp90 may indicate poor prognosis in some cases of GBM, considering that this chaperone can inhibit apoptosis [55].

GBMs are also characterized by neo-angiogenesis and invasion, which is a histopathological hallmark of these cancers associated with a worse prognosis [56,57]. We therefore examined the expression of the VEGFRs belonging to a superfamily of RTK (receptor tyrosine kinase) and considered key mediators of angiogenesis [58]. VEGFRs are augmented in grade IV glioma vasculature and grade IV glioma cells [59]. Previous studies found that VEGF and its corresponding receptors VEGFRs are significant prognostic factors for overall survival in patients with glioma [60]. Our results demonstrated positive VGFR-1 and VGFR-2 reactions with cytosol localization in the cell lines and a lower positive reaction for VEGFR-3 in the tumor biopsies. Previ-
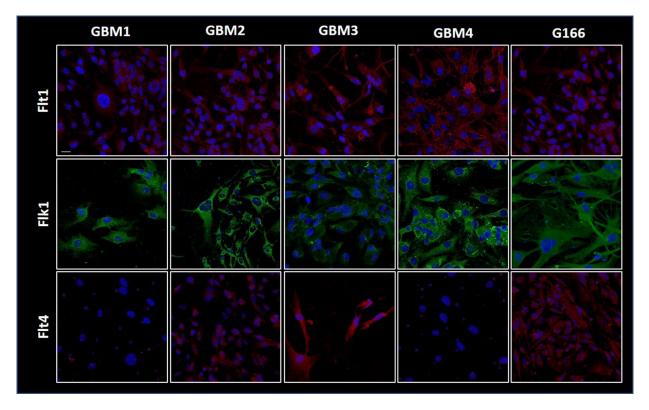
Fig. 6. Angiogenesis factors in the GBM cell lines. Immunofluorescence images for Flt1 (VEGFR-1), Flk1 (VEGFR-2), and Flt4 (VEGFR-3) showing their presence in the GBM and G166 cell lines. Specific primary antibodies for the receptors and secondary antibody conjugated with FITC (green fluorescence in the figure) or with TRITC (red fluorescence in the figure) were used, and the cell nuclei (blue) were stained with DAPI. Magnification $400\times$, scale bar 20 μm.

ous studies have shown that in normal brain a low or undetectable endothelial expression of VEGFR-2 can be found but in GBM it increases in parallel with tumor grade [61].

In summary, the levels of Hsp10, Hsp27, Hsp60, and Hsp90 were easily detectable in the GBM tumor tissue, even elevated some of them as compared with normal controls. In contrast, the levels of Hsp70 did not differ between the tumors and the normal tissue, being very low in all samples. These patterns of quantity and distribution of chaperones, if determined in many patients might, in the future, help in prognostication in GBM [60,62,63].

Our data provide a platform to elaborate a working hypothesis for future research, considering current knowledge about the CS and its roles in health and disease, including cancer. Hsp90 is a chaperone with a range of client proteins, including oncogene products (e.g., p53, AKT, RAF, EGFR, and MEK) involved in growth, survival, and cell-cycle regulatory pathways [64,65]. Hsp90 is upregulated within the hypoxic niche of human glioblastomas and a high level of Hsp90 is linked to the upregulation of HIF targets and CSC (cancer stem-like cells) marker genes [25] (Fig. 7).

Tumors with elevated Hsp90 had increased levels of the HIF target gene VEGF and high levels of the glioma stem-cells markers CD133 and nestin, supporting the notion that Hsp90 is activated by the CSC microenvironment [25]. Hsp90 and Hsp70 interact and regulate various tran-

scription factors, signaling molecules, and kinases that are related to cancer, including NF-κB, p53, and others [66] (Fig. 7, Ref. [67]). Hsp70 is induced by HSF1, which is the main factor involved in the transcription of Hsp70 [68]. A pathway that is upregulated during tumorigenesis is the HIF/VEGF signaling axis: tumor hypoxia and other stimuli induce HIF expression and subsequent activity, leading to angiogenesis [69]. Mediators of this pathway include HIF and VEGFRs [70], which are regulated by Hsp90 that binds to the c-terminal tail of VEGFR-2 [71]. Hsp90 also modulates downstream effectors of VEGF-dependent signaling pathways [72]. Ligand-induced homodimerization of VEGFR-2 leads to autophosphorylation of VEGFR-2 on tyrosine residues, which drives activation of major signaling pathways that include ERK, mitogen-activated protein kinases (MAP kinases) [73], and stress-activated protein kinase (e.g., SAPK2/p38) [74]. Once activated, the stress-activated protein kinase triggers phosphorylation of Hsp27, which initiates actin remodeling and actin-based motility [75] (Fig. 7). Hsp60 could enhance tumor progression by maintaining mitochondrial homeostasis and activating the mTOR signaling pathway—overactive in GBM—which increases tumor resistance to treatment [76]. We therefore hypothesize that by interfering with the activity of chaperones (negative chaperonotherapy [27,77], for example Hsp60 or Hsp90 it may be possible to stop GBM growth. This strat-
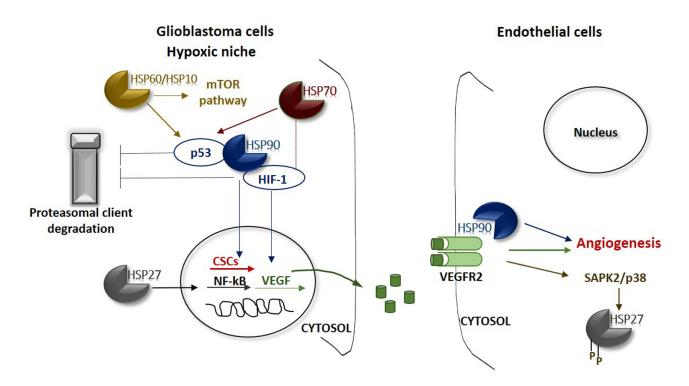
Fig. 7. Cartoon showing molecules and pathways that are relevant to the biology of GBM and could serve as a platform for a working hypothesis to be tested in search of specific targets, for instance chaperones, for anti-cancer compounds. Left panel; GBM cell. Hsp90 is at the center of pathways to maintain protein homeostasis, including interaction with protein degradations machineries that remove misfolded or otherwise defective proteins and generate building blocks, i.e., amino acids, for the new ones required in larger-than-normal amounts by cancer cells. Hsp90 also participates in tumorigenesis via the HIF/VEGF pathway. For example, hypoxia in the tumor mass induces HIF expression and activity, leading to VEGF production and angiogenesis. The chaperonins Hsp60 and Hsp10 are crucial for maintenance of the mitochondrial functional proteome and, thereby, ensure provision of energy to satisfy the needs of the tumor cell. In addition, Hsp70 and Hsp27 upregulate HIF activity increasing VEGF secretion. It is very likely that the CS, including the chaperones just mentioned, is key for chaperoning the protein molecules mediating the various pathways that are so important to satisfy the "greed" of the tumor cell for energy and proteins. The chaperones assist the tumor-cell proteins to mature and acquire a fully functional conformation and help them to translocate to the place in which they are to function. Therefore, components of the CS may be selected as targets for inhibition, namely negative chaperonotherapy, to hinder tumor survival and stop tumor growth and spread. Right panel; vascular endothelium cell. In vascular endothelial cells, Hsp90 interacts with members of the VEGF-regulated signaling pathway, including VEGFR2. A Hsp90/VEGFR2 complex exists in unstimulated endothelial cells [67]. However, binding of Hsp90 to VEGFR2 increases upon stimulation with VEGF, thus stimulating more angiogenesis. VEGF/VEGFR-2 promotes angiogenesis via a paracrine loop between cancer cells and vascular endothelial cells nearby. In addition, VEGFR-2 in vascular endothelial cells support tumor growth directly or through downstream activation of other signaling pathways, including the SAPK2/p38 pathway. The latter, once activated, triggers into action downstream molecules, such as Hsp27, which involves phosphorylation and stimulating actin remodeling and actin-based motility both necessary for angiogenesis. Hsp90 inhibition could alter the endothelial response and diminish or block angiogenesis by stimulating VEGFR2 proteolysis, providing another argument in favor of the use Hsp90 inhibitors as anti-cancer agents in GBM.

egy could be applied in combination with the standard treatment options such as surgery, irradiation, and chemotherapy.

5. Conclusions

In conclusion, GBM is a tumor that is still little known in many ways, very aggressive and resistant to current therapies. It is necessary to find new therapeutic strategies that can improve treatment and follow-up tools. New avenues for research on GBM have been opened by progression in the knowledge of the chaperone system (CS) and its functions as a physiological entity in health and disease, including tumors. In this study we conducted an immunomorphological evaluation in GBM tissue samples and cell lines of some molecular chaperones and some angiogenic factors to investigate on their role as biomarkers useful for differential

diagnosis, prognostication, and patient follow up. Therefore, on the one hand we wanted to provide useful details on the biology of GBM, on the other hand to add information that could be useful for the development of new therapeutic strategies. Finally, considering the current knowledge on CS and its roles in health and neoplastic diseases, we have developed a working hypothesis to be tested in search of specific targets, for instance chaperones, for anti-cancer drug compounds.

Author contributions

Ethics approval and consent to participate

Acknowledgment

Funding

Conflict of interest

References

[1] Louis DN, Perry A, Reifenberger G, von Deimling A, Figarella-Branger D, Cavenee WK, *et al*. The 2016 World Health Organization Classification of Tumors of the Central Nervous System: a summary. Acta Neuropathologica. 2016; 131: 803–820.

[2] Tateishi K, Wakimoto H, Cahill DP. IDH1 Mutation and World Health Organization 2016 Diagnostic Criteria for Adult Diffuse Gliomas: Advances in Surgical Strategy. Neurosurgery. 2017; 64: 134–138.

[3] Hattori N, Hirose Y, Sasaki H, Nakae S, Hayashi S, Ohba S, *et al*. World Health Organization grade II-III astrocytomas consist of genetically distinct tumor lineages. Cancer Science. 2016; 107: 1159–1164.

[4] Ebrahimi A, Skardelly M, Bonzheim I, Ott I, Mühleisen H, Eckert F, *et al*. ATRX immunostaining predicts IDH and H3F3a status in gliomas. Acta Neuropathologica Communications. 2016; 4: 60.

[5] Plate KH, Breier G, Weich HA, Mennel HD, Risau W. Vascular endothelial growth factor and glioma angiogenesis: Coordinate induction of VEGF receptors, distribution of VEGF protein and possible in vivo regulatory mechanisms. International Journal of Cancer. 1994; 59: 520–529.

[6] Lu-Emerson C, Duda DG, Emblem KE, Taylor JW, Gerstner ER, Loeffler JS, *et al*. Lessons from anti-vascular endothelial growth factor and anti-vascular endothelial growth factor receptor trials in patients with glioblastoma. Journal of Clinical Oncology. 2015; 33: 1197–1213.

[7] Gilbert MR, Dignam JJ, Armstrong TS, Wefel JS, Blumenthal DT, Vogelbaum MA, *et al*. A randomized trial of bevacizumab for newly diagnosed glioblastoma. The New England Journal of Medicine. 2014; 370: 699–708.

[8] Macario AJL, Conway de Macario E. Chaperone Proteins and Chaperonopathies. In Fink G. (ed.) Stress: Physiology, Biochemistry, and Pathology Handbook of Stress Series. Academic Press, Elsevier, San Diego CA, USA. 2019;135–152.

[9] Henderson B, Fares MA, Lund PA. Chaperonin 60: a paradoxical, evolutionarily conserved protein family with multiple moonlighting functions. Biological Reviews. 2013; 88: 955–987.

[10] Calderwood SK, Gong J. Heat Shock Proteins Promote Cancer: it's a Protection Racket. Trends in Biochemical Sciences. 2016; 41: 311–323.

[11] Saini J, Sharma PK. Clinical, Prognostic and Therapeutic Significance of Heat Shock Proteins in Cancer. Current Drug Targets. 2018; 19: 1478–1490.

[12] Cappello F, Mazzola M, Jurjus A, Zeenny M, Jurjus R, Carini F, *et al*. Hsp60 as a Novel Target in IBD Management: a Prospect. Frontiers in Pharmacology. 2019; 10: 26.

[13] Milani A, Basirnejad M, Bolhassani A. Heat-shock proteins in diagnosis and treatment: an overview of different biochemical and immunological functions. Immunotherapy. 2019; 11: 215–239.

[14] Macario AJL, Conway de Macario E. Chaperonins in cancer: Expression, function, and migration in extracellular vesicles. Seminars in Cancer Biology. 2021 Jun 1: S1044-579X(21)00159-0. doi: 10.1016/j.semcancer.2021.05.029. PMID: 34087417.

[15] Rappa F, Pitruzzella A, Marino Gammazza A, Barone R, Mocciaro E, Tomasello G, *et al*. Quantitative patterns of Hsps in tubular adenoma compared with normal and tumor tissues reveal the value of Hsp10 and Hsp60 in early diagnosis of large bowel cancer. Cell Stress & Chaperones. 2016; 21: 927–933.

[16] Fan W, Fan S, Feng J, Xiao D, Fan S, Luo J. Elevated expression of HSP10 protein inhibits apoptosis and associates with poor prognosis of astrocytoma. PLoS ONE. 2017; 12: e0185563.

[17] Choi S, Kam H, Kim K, Park SI, Lee Y. Targeting Heat Shock Protein 27 in Cancer: a Druggable Target for Cancer Treatment? Cancers. 2019; 11: 1195.

[18] Sheng B, Qi C, Liu B, Lin Y, Fu T, Zeng Q. Increased HSP27 correlates with malignant biological behavior of non-small cell lung cancer and predicts patient's survival. Scientific Reports. 2017; 7: 13807.

[19] Ernst BP, Wiesmann N, Gieringer R, Eckrich J, Brieger J. HSP27 regulates viability and migration of cancer cell lines following irradiation. Journal of Proteomics. 2020; 226: 103886.

[20] Castro GN, Cayado-Gutiérrez N, Zoppino FCM, Fanelli MA, Cuello-Carrión FD, Sottile M, *et al*. Effects of temozolomide (TMZ) on the expression and interaction of heat shock proteins (HSPs) and DNA repair proteins in human malignant glioma cells. Cell Stress & Chaperones. 2015; 20: 253–265.

[21] Alexiou G, Karamoutsios A, Lallas G, Ragos V, Goussia A, Kyritsis A, *et al*. Expression of heat shock proteins in brain tumors. Turkish Neurosurgery. 2014; 24: 745–749.

[22] Beaman GM, Dennison SR, Chatfield LK, Phoenix DA. Reliability of HSP70 (HSPA) expression as a prognostic marker in

glioma. Molecular and Cellular Biochemistry. 2014; 393: 301–307.

[23] Chen S, Yin C, Lao T, Liang D, He D, Wang C, *et al*. AMPK-HDAC5 pathway facilitates nuclear accumulation of HIF-1α and functional activation of HIF-1 by deacetylating Hsp70 in the cytosol. Cell Cycle. 2015; 14: 2520–2536.

[24] Schopf FH, Biebl MM, Buchner J. The HSP90 chaperone machinery. Nature Reviews Molecular Cell Biology. 2017; 18: 345–360.

[25] Filatova A, Seidel S, Böğürcü N, Gräf S, Garvalov BK, Acker T. Acidosis Acts through HSP90 in a PHD/VHL-Independent Manner to Promote HIF Function and Stem Cell Maintenance in Glioma. Cancer Research. 2016; 76: 5845–5856.

[26] Macario AJL, Conway de Macario E. Sick chaperones, cellular stress, and disease. The New England Journal of Medicine. 2005; 353: 1489–1501.

[27] Macario AJL, Conway de Macario E. Chaperonopathies and chaperonotherapy. FEBS Letters. 2007; 581: 3681–3688.

[28] Cappello F, Marino Gammazza A, Palumbo Piccionello A, Campanella C, Pace A, Conway de Macario E, *et al*. Hsp60 chaperonopathies and chaperonotherapy: targets and agents. Expert Opinion on Therapeutic Targets. 2014; 18: 185–208.

[29] Rappa F, Sciume C, Lo Bello M, Bavisotto CC, Marino Gammazza A, Barone R, *et al*. Comparative analysis of Hsp10 and Hsp90 expression in healthy mucosa and adenocarcinoma of the large bowel. Anticancer Research. 2014; 34: 4153–4159.

[30] Preston AN, Cervasio DA, Laughlin ST. Visualizing the brain's astrocytes. Methods in Enzymology. 2019; 622: 129–151.

[31] Vinci L, Ravarino A, Fanos V, Naccarato AG, Senes G, Gerosa C, *et al*. Immunohistochemical markers of neural progenitor cells in the early embryonic human cerebral cortex. European Journal of Histochemistry. 2016; 60: 2563.

[32] Abbassi RH, Recasens A, Indurthi DC, Johns TG, Stringer BW, Day BW, *et al*. Lower Tubulin Expression in Glioblastoma Stem Cells Attenuates Efficacy of Microtubule-Targeting Agents. ACS Pharmacology & Translational Science. 2019; 2: 402–413.

[33] Isgrò MA, Bottoni P, Scatena R. Neuron-Specific Enolase as a Biomarker: Biochemical and Clinical Aspects. Advances in Experimental Medicine and Biology. 2015; 867: 125–143.

[34] Rappa F, Cappello F, Halatsch M, Scheuerle A, Kast RE. Aldehyde dehydrogenase and HSP90 co-localize in human glioblastoma biopsy cells. Biochimie. 2013; 95: 782–786.

[35] Rappa F, Unti E, Baiamonte P, Cappello F, Scibetta N. Different immunohistochemical levels of Hsp60 and Hsp70 in a subset of brain tumors and putative role of Hsp60 in neuroepithelial tumorigenesis. European Journal of Histochemistry. 2013; 57: e20.

[36] Hoter A, Rizk S, Naim HY. The Multiple Roles and Therapeutic Potential of Molecular Chaperones in Prostate Cancer. Cancers. 2019; 11: 1194.

[37] Lang BJ, Guerrero-Giménez ME, Prince TL, Ackerman A, Bonorino C, Calderwood SK. Heat Shock Proteins Are Essential Components in Transformation and Tumor Progression: Cancer Cell Intrinsic Pathways and Beyond. International Journal of Molecular Sciences. 2019; 20: 4507.

[38] Siebert C, Ciato D, Murakami M, Frei-Stuber L, Perez-Rivas LG, Monteserin-Garcia JL, *et al*. Heat Shock Protein 90 as a Prognostic Marker and Therapeutic Target for Adrenocortical Carcinoma. Frontiers in Endocrinology. 2019; 10: 487.

[39] Saha T, van Vliet AA, Cui C, Macias JJ, Kulkarni A, Pham LN, *et al*. Boosting Natural Killer Cell Therapies in Glioblastoma Multiforme Using Supramolecular Cationic Inhibitors of Heat Shock Protein 90. Frontiers in Molecular Biosciences. 2021; 8:754443.

[40] Gimenez M, Marie SKN, Oba-Shinjo S, Uno M, Izumi C, Oliveira JB, *et al*. Quantitative proteomic analysis shows differentially expressed HSPB1 in glioblastoma as a discriminating short from long survival factor and NOVA1 as a differentiation factor between low-grade astrocytoma and oligodendroglioma. BMC Cancer. 2015; 15: 481.

[41] Cappello F, David S, Rappa F, Bucchieri F, Marasà L, Bartolotta TE, *et al*. The expression of HSP60 and HSP10 in large bowel carcinomas with lymph node metastase. BMC Cancer. 2005; 5: 139.

[42] Basset CA, Rappa F, Lentini VL, Barone R, Pitruzzella A, Unti E, *et al*. Hsp27 and Hsp60 in human submandibular salivary gland: Quantitative patterns in healthy and cancerous tissues with potential implications for differential diagnosis and carcinogenesis. Acta Histochemica. 2021; 123: 151771.

[43] Ramp U, Mahotka C, Heikaus S, Shibata T, Grimm MO, Willers R, *et al*. Expression of heat shock protein 70 in renal cell carcinoma and its relation to tumor progression and prognosis. Histology and Histopathology. 2007; 22: 1099–107.

[44] Park CS, Joo IS, Song SY, Kim DS, Bae DS, Lee JH. An immunohistochemical analysis of heat shock protein 70, p53, and estrogen receptor status in carcinoma of the uterine cervix. Gynecologic Oncology. 1999; 74: 53–60.

[45] Boonjaraspinyo S, Boonmars T, Kaewkes S, Laummaunwai P, Pinlaor S, Loilome W, *et al*. Down-regulated expression of HSP70 in correlation with clinicopathology of cholangiocarcinoma. Pathology Oncology Research. 2012; 18: 227–237.

[46] Lobinger D, Gempt J, Sievert W, Barz M, Schmitt S, Nguyen HT, *et al*. Potential Role of Hsp70 and Activated NK Cells for Prediction of Prognosis in Glioblastoma Patients. Frontiers in Molecular Biosciences. 2021; 8: 669366.

[47] Di K, Keir ST, Alexandru-Abrams D, Gong X, Nguyen H, Friedman HS, *et al*. Profiling Hsp90 differential expression and the molecular effects of the Hsp90 inhibitor IPI-504 in high-grade glioma models. Journal of Neuro-Oncology. 2014; 120: 473–481.

[48] Siegelin MD, Habel A, Gaiser T. 17-AAG sensitized malignant glioma cells to death-receptor mediated apoptosis. Neurobiology of Disease. 2009; 33: 243–249.

[49] Sauvageot CM, Weatherbee JL, Kesari S, Winters SE, Barnes J, Dellagatta J, *et al*. Efficacy of the HSP90 inhibitor 17-AAG in human glioma cell lines and tumorigenic glioma stem cells. Neuro-Oncology. 2009; 11: 109–121.

[50] Wang J, Cui S, Zhang X, Wu Y, Tang H. High expression of heat shock protein 90 is associated with tumor aggressiveness and poor prognosis in patients with advanced gastric cancer. PLoS ONE. 2013; 8: e62876.

[51] Kim K, Lee HW, Lee EH, Park MI, Lee JS, Kim MS, *et al*. Differential expression of HSP90 isoforms and their correlations with clinicopathologic factors in patients with colorectal cancer. International Journal of Clinical and Experimental Pathology. 2019; 12: 978–986.

[52] Lomeli N, Bota DA. Targeting HSP90 in malignant gliomas: onalespib as a potential therapeutic. Translational Cancer Research. 2018; 7: 6215–6226.

[53] Orth M, Albrecht V, Seidl K, Kinzel L, Unger K, Hess J, *et al*. Inhibition of HSP90 as a Strategy to Radiosensitize Glioblastoma: Targeting the DNA Damage Response and Beyond. Frontiers in Oncology. 2021; 11: 612354.

[54] Basset CA, Cappello F, Rappa F, Lentini VL, Jurjus AR, Conway de Macario E, *et al*. Molecular chaperones in tumors of salivary glands. Journal of Molecular Histology. 2020; 51: 109–115.

[55] Li D, Marchenko ND, Moll UM. SAHA shows preferential cytotoxicity in mutant p53 cancer cells by destabilizing mutant p53 through inhibition of the HDAC6-Hsp90 chaperone axis. Cell Death and Differentiation. 2011; 18: 1904–1913.

[56] Schiffer D, Annovazzi L, Casalone C, Corona C, Mellai M.

Glioblastoma: Microenvironment and Niche Concept. Cancers. 2018; 11: 5.

[57] Lombardi G, De Salvo GL, Brandes AA, Eoli M, Rudà R, Faedi M, *et al*. Regorafenib compared with lomustine in patients with relapsed glioblastoma (REGOMA): a multicentre, open-label, randomised, controlled, phase 2 trial. The Lancet Oncology. 2019; 20: 110–119.

[58] Shibuya M. Vascular Endothelial Growth Factor (VEGF) and its Receptor (VEGFR) Signaling in Angiogenesis: a Crucial Target for Anti- and Pro-Angiogenic Therapies. Genes & Cancer. 2011; 2: 1097–1105.

[59] Rainer E, Wang H, Traub-Weidinger T, Widhalm G, Fueger B, Chang J, *et al*. The prognostic value of [123i]-vascular endothelial growth factor ([123i]-VEGF) in glioma. European Journal of Nuclear Medicine and Molecular Imaging. 2018; 45: 2396–2403.

[60] Tang H, Li J, Liu X, Wang G, Luo M, Deng H. Down-regulation of HSP60 Suppresses the Proliferation of Glioblastoma Cells via the ROS/AMPK/mTOR Pathway. Scientific Reports. 2016; 6: 28388.

[61] Jaal J, Kase M, Minajeva A, Saretok M, Adamson A, Junninen J, *et al*. VEGFR-2 Expression in Glioblastoma Multiforme Depends on Inflammatory Tumor Microenvironment. International Journal of Inflammation. 2015; 2015: 385030.

[62] van Ommeren R, Staudt MD, Xu H, Hebb MO. Advances in HSP27 and HSP90-targeting strategies for glioblastoma. Journal of Neuro-Oncology. 2016; 127: 209–219.

[63] Chen H, Gong Y, Ma Y, Thompson RC, Wang J, Cheng Z, *et al*. A Brain-Penetrating Hsp90 Inhibitor NXD30001 Inhibits Glioblastoma as a Monotherapy or in Combination With Radiation. Frontiers in Pharmacology. 2020; 11: 974.

[64] Walerych D, Kudla G, Gutkowska M, Wawrzynow B, Muller L, King FW, *et al*. Hsp90 chaperones wild-type p53 tumor suppressor protein. The Journal of Biological Chemistry. 2004; 279: 48836–48845.

[65] Liu H, Lu Z, Shi X, Liu L, Zhang P, Golemis EA, *et al*. HSP90 inhibition downregulates DNA replication and repair genes via E2F1 repression. Journal of Biological Chemistry. 2021; 297: 100996.

[66] Lanneau D, Brunet M, Frisan E, Solary E, Fontenay M, Garrido C. Heat shock proteins: essential proteins for apoptosis regulation. Journal of Cellular and Molecular Medicine. 2008; 12:

743–761.

[67] Masson-Gadais B, Houle F, Laferrière J, Huot J. Integrin alphavbeta3, requirement for VEGFR2-mediated activation of SAPK2/p38 and for Hsp90-dependent phosphorylation of focal adhesion kinase in endothelial cells activated by VEGF. Cell Stress & Chaperones. 2003; 8: 37–52.

[68] Antonietti P, Linder B, Hehlgans S, Mildenberger IC, Burger MC, Fulda S, *et al*. Interference with the HSF1/HSP70/BAG3 Pathway Primes Glioma Cells to Matrix Detachment and BH3 Mimetic-Induced Apoptosis. Molecular Cancer Therapeutics. 2017; 16: 156–168.

[69] Balamurugan K. HIF-1 at the crossroads of hypoxia, inflammation, and cancer. International Journal of Cancer. 2016; 138: 1058–1066.

[70] Kaur B, Khwaja FW, Severson EA, Matheny SL, Brat DJ, Van Meir EG. Hypoxia and the hypoxia-inducible-factor pathway in glioma growth and angiogenesis. Neuro-Oncology. 2005; 7: 134–153.

[71] Le Boeuf F, Houle F, Huot J. Regulation of vascular endothelial growth factor receptor 2-mediated phosphorylation of focal adhesion kinase by heat shock protein 90 and Src kinase activities. The Journal of Biological Chemistry. 2004; 279: 39175–39185.

[72] Bohonowych JE, Gopal U, Isaacs JS. Hsp90 as a gatekeeper of tumor angiogenesis: clinical promise and potential pitfalls. Journal of Oncoslogy. 2010; 2010: 412985.

[73] Szabo E, Schneider H, Seystahl K, Rushing EJ, Herting F, Weidner KM, *et al*. Autocrine VEGFR1 and VEGFR2 signaling promotes survival in human glioblastoma models in vitro and in vivo. Neuro-Oncology. 2016; 18: 1242–1252.

[74] Deschesnes RG, Huot J, Valerie K, Landry J. Involvement of p38 in apoptosis-associated membrane blebbing and nuclear condensation. Molecular Biology of the Cell. 2001; 12: 1569–1582.

[75] Shiryaev A, Dumitriu G, Moens U. Distinct roles of MK2 and MK5 in cAMP/PKA- and stress/p38MAPK-induced heat shock protein 27 phosphorylation. Journal of Molecular Signaling. 2011; 6: 4.

[76] Tang H, Li J, Liu X, Wang G, Luo M, Deng H. Down-regulation of HSP60 Suppresses the Proliferation of Glioblastoma Cells via the ROS/AMPK/mTOR Pathway. Scientific Reports. 2016; 6: 28388.

[77] Macario AJL, Conway de Macario E. Chaperonopathies by defect, excess, or mistake. Annals of the New York Academy of Sciences. 2007; 1113: 178–191.